Kristofer K. Kloehn[1], **Timothy J. Beechie, Sarah A. Morley,** and **Holly J. Coe,** NOAA Fisheries, Northwest Fisheries Science Center, 2725 Montlake Boulevard East, Seattle, Washington 98112

and

Jeffrey J. Duda, U.S. Geological Survey, Western Fisheries Research Center, 6505 NE 65th Street, Seattle, Washington 98115

Influence of Dams on River-Floodplain Dynamics in the Elwha River, Washington

Abstract

The Elwha dam removal project presents an ideal opportunity to study how historic reduction and subsequent restoration of sediment supply alter river-floodplain dynamics in a large, forested river floodplain. We used remote sensing and onsite data collection to establish a historical record of floodplain dynamics and a baseline of current conditions. Analysis was based on four river reaches, three from the Elwha River and the fourth from the East Fork of the Quinault River. We found that the percentage of floodplain surfaces between 25 and 75 years old decreased and the percentage of surfaces >75 years increased in reaches below the Elwha dams. We also found that particle size decreased as downstream distance from dams increased. This trend was evident in both mainstem and side channels. Previous studies have found that removal of the two Elwha dams will initially release fine sediment stored in the reservoirs, then in subsequent decades gravel bed load supply will increase and gradually return to natural levels, aggrading river beds up to 1 m in some areas. We predict the release of fine sediments will initially create bi-modal grain size distributions in reaches downstream of the dams, and eventual recovery of natural sediment supply will significantly increase lateral channel migration and erosion of floodplain surfaces, gradually shifting floodplain age distributions towards younger age classes.

Introduction

The Elwha River dam removal project presents an ideal opportunity to study how historical anthropogenic reduction and future restoration of sediment supply alter river-floodplain dynamics in a large, forested river floodplain. The Glines Canyon and Elwha Dams segregate the Elwha River into three distinct reaches, two with reduced sediment supply (one below the dams and one between the dams) and one with natural sediment supply (above both dams). Sediment supply to the two reaches downstream of dams has been reduced for more than 80 years, which typically results in bed coarsening and channel incision (Ligon et al. 1995, Pizzuto 2002, Grant et al. 2003). Indeed, bed coarsening has been detected downstream of the Elwha dams (Pohl 2004), yet it remains unclear how this change has altered channel-floodplain dynamics, river morphology, and consequently biology.

The purposes of this paper are twofold. First, we describe the use of historical aerial photography to evaluate river-floodplain dynamics, and illustrate how river-floodplain dynamics have changed over the last 60 years in dammed and undammed river reaches. Second, we use field data to compare size distributions of river-bed sediments in dammed and undammed reaches to document how dam placement has altered river-bed grain sizes. Results of this study provide a baseline characterization of current river-floodplain dynamics and bed character, as well as a basis for predicting physical and biological responses of river-floodplain dynamics to dam removal and restoration of a natural sediment supply regime.

Study Area

The Elwha River drains an area of 833 km^2 in the Olympic Mountains of Washington State, USA (Figure 1), with 83% of the watershed inside the boundaries of Olympic National Park (BOR 1996a). The central Olympic Mountains rise to an elevation of over 2400 m, and are comprised of sedimentary and metamorphic rocks of marine origin (sandstone, schist, and shale; Tabor 1975). Surrounding the central mountains is the Crescent Formation, a series of marine basalts and sandstones. At the northern edge of the Olympic Peninsula are 100-m thick deposits of unconsolidated sediments of glacial origin. As the Elwha River emerges from the core of the Olympic Mountains

[1]Author to whom correspondence should be addressed.
E-mail address: kloehnk@uvic.ca

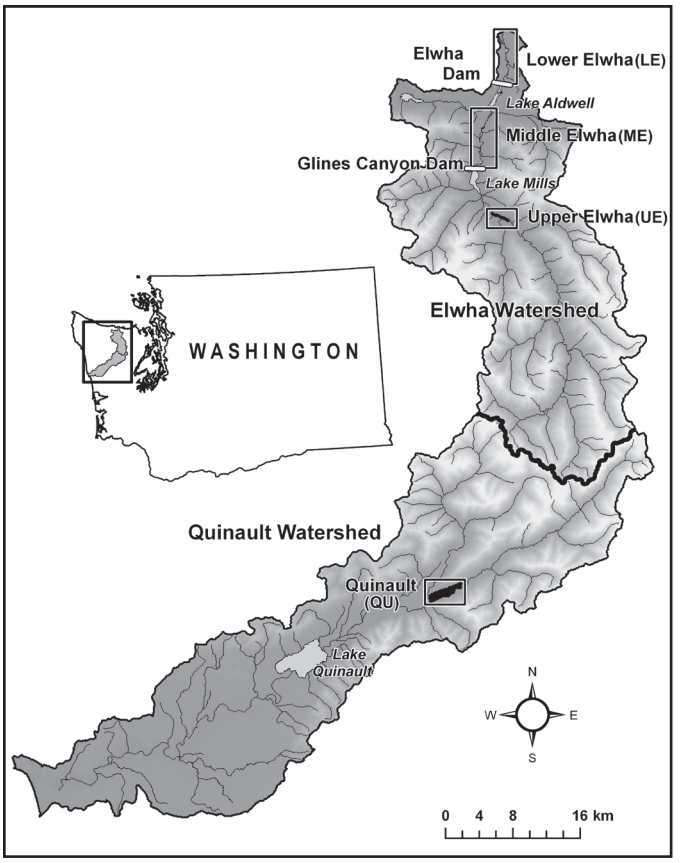

Figure 1. Map of the Elwha and Quinault basins with reach locations highlighted.

it flows through alternating canyon and valley reaches, reflecting differences in erosion resistance of each rock type. Average annual rainfall ranges from 100 cm·yr^{-1} near Port Angeles to over 550 cm·yr^{-1} in the headwaters. Vegetation ranges from alpine tundra and subalpine parklands at high elevations to dense conifer forests in the Western Hemlock (*Tsuga heterophylla)* zone at low elevations (Franklin and Dyrness 1973). Floodplains of the Elwha River are populated with red alder (*Alnus rubra*), big leaf maple (*Acer macrophyllum*), black cottonwood (*Populus balsamifera* ssp. *trichocarpa*), grand fir (*Abies grandis*), and willow species (*Salix* spp.). Coniferous forest species include Douglas fir (*Pseudotsuga menziesii*), western hemlock, western red cedar (*Thuja plicata*), silver fir (*Abies amabilis*) and subalpine fir (*Abies lasiocarpa*).

Elwha Dam, constructed in 1912 at river kilometer 7.9, is 34 meters high and has trapped an estimated 3.0 million m^3 of sediment in its reservoir, Lake Aldwell (BOR 1995). Glines Canyon Dam, constructed in 1925 at river kilometer 21.6, is 64 meters high and has stored over 10.6 million m^3 of sediment beneath Lake Mills. Sand and finer materials comprise 85% of the sediments beneath the Glines Canyon Dam reservoir and 95% of the sediments beneath the Elwha Dam reservoir. Gravel and coarser materials are confined to river deltas at the head of each reservoir (BOR 1995). The planned dam removal project allows river erosion of reservoir sediments and proposes no actions to remove or stabilize those sediments before or after dam removal (BOR 1996b). Deconstruction of the two dams is expected to take two years (BOR 1996a). Erosion of reservoir sediment is expected to be rapid during the first two years and then slow dramatically after 2 to 5 years (BOR 1996b).

We focused upon four study reaches. A site above the upper Elwha dam and a site in the Quinault River valley were reference reaches whereas the sites below the Glines Canyon dam and below the Elwha dam were response reaches (Figure 1). All four reaches have unconfined floodplains with estimated two-year flood discharges between 300 and 400 m^{3}s^{-1}. One reference reach was the Geyser Valley section of the Elwha River located upstream of the Glines Canyon dam (hereafter, the UE, Figure 2). However, this reach has chronically high bed-load sediment supply caused by persistent terrace erosion since 1967 (Acker et al. 2008) and a significantly steeper slope than the two downstream reaches (Table 1). Therefore, we searched other Olympic Peninsula river basins for a second reference reach with slope and discharge more similar to the Lower Elwha reach. A reach of the Quinault River immediately upstream of the Olympic National Park boundary (hereafter, the QU) was most similar to the Elwha reaches downstream of the dams. The two response reaches (hereafter referred to as the LE and ME reaches) have additional infrastructure constraining the river channels including short sections of rip-

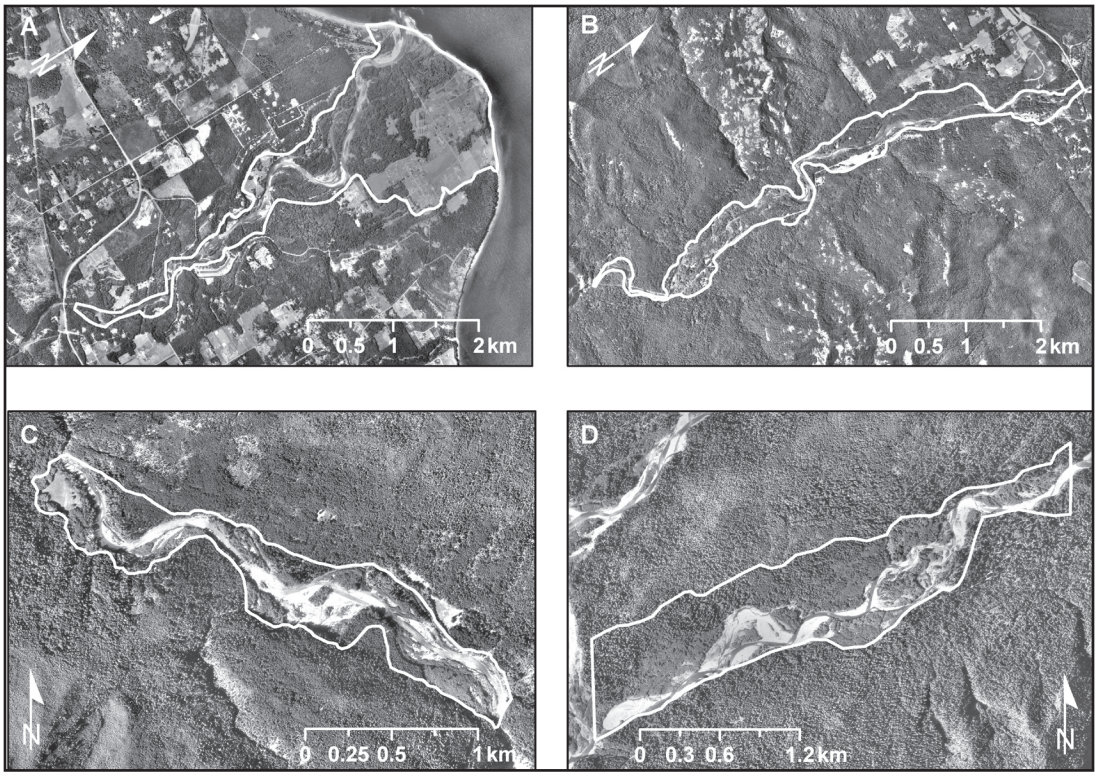

Figure 2. Detail photos of (A) LE, (B) ME, (C) UE, and (D) QU study reaches.

rap, set-back levees, and one low-head diversion structure. The average bankfull width of the study reaches was 68 m (LE), 89 m (ME), 63 m (QU), and 115 m (UE).

Sediment transport modeling using HEC-6 (USACOE 1993) suggests that aggradation of channel beds downstream of the dams will be confined to pools during the first three years following dam removal because fine sediments initially eroded from the reservoir will be transported through the riffle reaches (BOR 1996b). Aggradation is expected to be less in ME than in LE because river sediment transport capacity is higher in the steeper ME. The initial wave of fine sediments is expected to temporarily fill pools, but not to raise the entire bed (BOR 1996b). Gravel and coarser sediments from reservoir deltas are predicted to arrive in the LE reach after several decades, and are expected to cause bed aggradation averaging about 1 m after 50 yrs (BOR 1996b).

TABLE 1. Channel characteristics of study reaches in the Elwha and Quinault Rivers.

Reach Location	LE Below dams	ME Between dams	UE Above dams	QU No dams
Bankfull channel width (m)	89	68	115	63
Channel slope (m/m)	0.0030	0.0065	0.0149	0.0043
Side channel length (km)	6.7	8.7	3.5	12.5
Main channel length (km)	7.9	13.0	6.9	4.8
SC/MC ratio	0.848	0.669	0.507	2.604

Natural sediment supply from the upper Elwha River basin delivered to Lake Mills since 1927, when Glines Canyon Dam was built, has been about 146 $m^3 km^{-2} yr^{-1}$ (BOR 1996b).

Methods

We documented temporal changes in floodplain surface age by classifying vegetation age at fixed points throughout a time series of aerial photographs. Vegetation age was used as a surrogate for estimating the age of the floodplain surface it occupied. We used vegetation age classes estimated from the regression of mean crown diameter to stand age ($R^2 = 0.93$; Beechie et al. 2006). These classes provided a range of crown diameter measurements coupled with a range of vegetation ages.

With the basic methodology in place we collected all available aerial photographs and calibration reports for each of our study reaches (Table 2). Calibration reports contain information about the camera and flight associated with the photographs. This information is required to orthorectify a photograph and proved to be a limiting factor in several instances. Ideally, a time series would provide equal coverage of all sites, a range that encompasses all classes of vegetation succession and an interval or frequency that captures a system's turnover of young vegetation classes. However, ideal coverage was not required and the availability of photographs and calibration reports ultimately determined the range and interval of years available for our analysis (Table 2).

Each photograph was scanned at a minimum of 600 dpi, saved in tagged image file format (.tif), and either orthorectified using ERDAS Imagine 8.6 software with the Orthobase extension, or georeferenced in ArcInfo 9.1 GIS software. The orthorectification process required a minimum of two photographs with approximately 30 % overlap, a digital elevation model (DEM) of the coverage area, and at minimum the calibrated focal length of the source camera. The majority of images did not have calibration reports; these reports were located separately based on the limited information displayed on the images themselves (i.e., frame number, project number, scale and year).

We used reference images as the basis for associating spatial coordinates with our scanned images. Reference images were USGS 7.5-minute digital orthophoto quadrangles (DOQs), which meet National Map Accuracy Standards of ± 40 feet horizontal accuracy for 90 % of points tested (USGS 1996). The relative accuracy of each orthophoto was reflected by the root mean square error (RMSE)—a value generated by calculating the square root of the average of the squared differences between generated values (x and y coordinates) and the actual values of station points or reference images (x and y coordinates) (USGS 1996). Reference images were from 1990 (RMSE = 1.7 m) and 1994 (RMSE = 2.8 m) for the LE, 1990 (RMSE = 2.0 m) for the UE and ME, and 1994 (RMSE = 1.3 m) for the QU. We used USGS 7.5-minute DEM with a maximum RMSE of 7 m.

TABLE 2. Aerial photographs used in this study.

	Photo		Reach			
Year	Scale	BW/ Color	Lower Elwha	Middle Elwha	Upper Elwha	Quinault reference
1939		BW				
1943		BW		X		
1953		BW				
1956		BW	X			
1965		BW	X			
1968		BW		*X	X	
1971		BW	X			
1976	1:24,000	Color		**X	X	X
1977		BW	X			
1981		BW		X	X	X
1990	1:12,000	BW	X		X	X
1994	1:12,000	BW	X	X		
2000	1:12,000	BW		X	X	X

*15 points missing due to incomplete coverage
**23 points missing due to incomplete coverage

Scanned images were imported into ERDAS Imagine where ground control points (GCPs) were placed at locations identifiable on both the reference photo and the scanned aerial photo. Where possible, GCPs were placed at each corner, in the center and at the midpoints of each side of the scanned images. In addition to GCPs, tie points were placed on the overlapping portions of each image. Based on the GCPs and tie points, the Orthobase 'AutoTie' function generated a user-specified number of additional tie points. We generated a minimum of 80 'AutoTie' points for each scanned image in a coverage area. In the event that suitable GCPs could not be located at each of the prescribed areas, points were chosen in alternate locations or omitted. In either situation, the RMSE and photographs were inspected visually to ensure protocol standards were met. This process was repeated for each scanned image. Orthorectified images were combined using the ERDAS Imagine "Mosaic" tool and then exported as a single 'imagine' (.img) formatted file. This orthorectification process was used for the QU, LE and UE reaches.

Aerial photography of the ME reach was georeferenced in ArcInfo 9.1 rather than undergoing the orthorectification process. This change in methods resulted from limited access to the ERDAS Imagine Orthobase extension required to orthorectify photographs. Georeferencing is similar to orthorectifying in its use of ground control points to associate spatial coordinates of a reference image to another image. Unlike orthorectification, georeferencing with ArcInfo 9.1 does not associate elevation data, generate 'AutoTie' points or utilize camera or flight information. As a result, georeferenced images were more susceptible to spatial error. We found that careful placement of control points, coupled with a thorough visual inspection of each image (displayed at a scale of 1:1,500), produced accurate results. We used the RMSE generated for each of the ground control points and several tools within ArcInfo 9.1 to visually inspect each transformation.

Once all photos were either orthorectified or georeferenced, they were imported into the geographic information system (GIS), ArcInfo 9.1. We used USGS 3.5-minute topographic quarter quadrangles, digital orthophoto quadrangles, aerial photographs and field surveys to create a polygon shapefile delineating the floodplain area of each study reach. Using ArcInfo 9.1, we generated a grid over the floodplain area with a minimum of 190 intersections within each floodplain. Each intersection was converted to a point feature and assigned a unique identification number. These point features served as a sample points for classifying vegetation age.

We developed a sampling protocol which selected for maximum vegetation age and minimized sampling error associated with image variability. Maximum vegetation age was used to establish the maximum age of the surface on which it was located; additionally, it reduced occurrences of negative growth rates caused by variations between images' spatial accuracy, resolution and source angle. At each point, we identified and measured the largest crown within 20 meters of the sample point. We used a 20 meter sampling area to account for variation in spatial accuracy. Points located on the border of two age classes were associated with the age class that composed the majority of the sampling area. To account for bias, this protocol was suspended when a point was located in the active channel. Because crown diameter is correlated with surface age, we then classified each point following Beechie et al. (2006): C = active channel, V_1 = newly established vegetation (<5 yrs old), V_2 = vegetation with a crown size < 5 m (5-25 yrs old), V_3 = vegetation with a crown size > 5 m but < 10 m (25-75 yrs old), and V_4 = vegetation with a crown size > 10 m (>75 yrs old). Vegetation obscured by shadows, poor photo resolution or distortion were classified accordingly, and omitted from the analysis. Points falling in areas dominated by grasses or other non-forest cover were classified as "Other" because surface age could not be determined.

We characterize channel-floodplain dynamics at each site based on the distribution of surface ages through time. For each reach we calculate the average age of floodplain surfaces (age_{mean}).

$$age_{mean} = \frac{3C_{V1} + 15C_{V2} + 50C_{V3} + 150C_{V4}}{C_{Total} - C_C} \quad (1)$$

where $C_{V1\text{-}4}$ are the number of sample points in classes V1 through V4, C_c is the number of sample points in channel, and C_{Total} is the total number of sample points. Values of 3, 15, 50, and 150 are approximate midpoint ages of vegetation classes. We calculated mean erosion return intervals (ERI; Beechie et al. 2006), which represent the average length of time that a sample point spends

as a floodplain surface before being reoccupied by the channel, based on the equation of Booth (1991);

$$\sum f_t = 1 - e^{-pt} \quad (2)$$

where f_t is the cumulative proportion of floodplain surfaces less than age t, p is the estimated probability of erosion by the channel in any one year, and the average time between disturbances is $1/p$. We calculated evenness (E) of the five cover classes

$$E = \frac{H'}{H_{\max}} = \frac{-\sum p_i \ln(p_i)}{\ln(s)} \quad (3)$$

where H′ is the Shannon-Weiner diversity index, H_{max} is the maximum value of the diversity index, p_i is the proportion of the ith cover class, and s is the number of cover classes (Pielou 1977). Evenness is an index ranging from zero to one, where zero indicates complete coverage by a single cover class and one indicates equal proportions of all cover types. We used linear regression analysis to estimate trends in proportions of each age class, and for temporal trends in the metrics of floodplain dynamics.

We characterized the morphology of each of the four study reaches by measuring slope from USGS 7.5-minute topographic maps, and by measuring bankfull channel width, side channel locations, and stream bed particle sizes in the field (Table 1). Bankfull channel widths were measured at eight or more cross sections in each reach, and averaged. Side channels were mapped in the field using a combination of aerial photography and GPS locations. GPS points were difficult to acquire in these steep-walled valleys, so most channels were drawn on recent aerial photos and later digitized. Wolman pebble counts of 100 particles were used to measure streambed particle sizes in several riffles distributed longitudinally throughout each of our study reaches (Wolman 1954). All field measurement points and channel locations were digitized and combined in GIS (Table 1). We calculated a slope-width index from reach slopes and the bankfull width measurements associated with each pebble count site. The slope-width index is proportional to stream power via the relationship between bankfull discharge and channel width (Leopold et al. 1964), and it is a predictor of both bed material size and sediment discharge (Richards 1982). The cumulative percentages of various particle size classes (<64 mm, <128mm, and <256 mm) were then plotted against these index values in order to compare grain sizes among reaches while correcting for differences in stream competence (a measure of particle sizes that a river can move during a bankfull flood). We also used regression analysis to examine downstream trends in particle sizes. We regressed wolman pebble count data against distance downstream from the Elwha (LE) and Glines Canyon (ME) dams. To develop similar data for the control reaches, we arbitrarily located a point 1 km upstream from the uppermost pebble count survey in the Quinault and UE reaches.

Results

The ME was the most stable of the response reaches with 41.51% of the floodplain >75 yrs old, an ERI of 49 yrs, and a probability of erosion at a point in any one year of 0.020 (Table 3).

TABLE 3. Summaries of vegetation and floodplain surface age metrics from the four reaches of the Elwha and Quinault Rivers based on aerial photo analysis.

Reach	LE	ME	UE	QU
Mean % channel	7.39	20.67	30.65	17.01
Mean % of floodplain <5 yrs old	0.40	1.97	1.66	3.62
Mean % of floodplain >75 yr old	27.15	41.51	26.31	47.12
Mean age of floodplain surfaces (yrs)	72.6	99.3	84.7	103.3
Probability of erosion at a point in any year	0.021*	0.020**	0.031**	0.019**
Erosion return interval (yrs)	48*	49**	32**	53**
Evenness	0.74*	0.69**	0.73**	0.73**

*Analysis based on single aerial photograph: 1994.
**Analysis based on single aerial photograph: 2000.

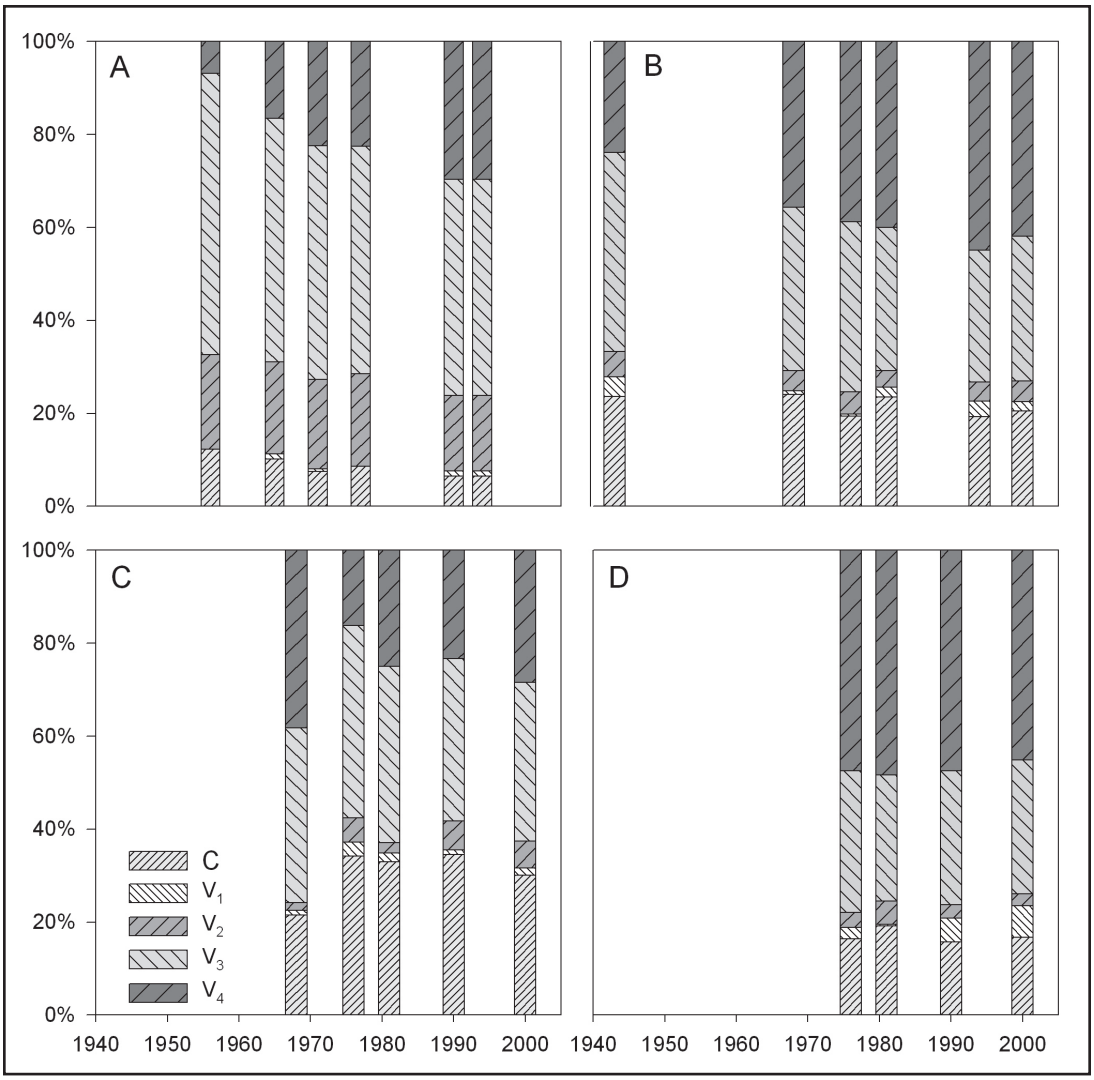

Figure 3. Age composition of floodplain surfaces through time in the (A) LE, (B) ME, (C) UE, and (D) QU study reaches. Surface categories were channel (C), surface <5yrs old (V_1), surface 5-25 yrs old (V_2), surface 25-75 yrs old (V_3), and surface >75 yrs old (V_4).

The UE was the most dynamic of all the study reaches (Table 3) with the highest ERI (32 yrs), the lowest percentage of floodplain surfaces >75 yrs old (26.31%), and the highest probability of erosion at a point in any one year (0.031). The QU reference reach was most stable of all the study reaches (Table 3) with the longest ERI (53 yrs), the greatest percentage of floodplain >75 yrs old (47.12%), and the lowest probability of erosion at a point in any one year (0.019). Additionally, the QU reach had the most stable distribution of age classes through time (Figure 3) and the highest mean age of floodplain surfaces (103.3 yrs) of all the study reaches (Table 3). Evenness values were similar for all reaches.

Analysis of vegetation age showed a statistically significant trend of transition from younger to older age classes downstream of each dam (Table 4). In the LE and ME percentages of vegetation >75 yrs old (V_4) increased as the time series progressed, while percentages of vegetation younger than 75 years old ($V_1 - V_3$) generally decreased or remained static (Figure 3). The statistical significance of these trends was limited to the increase in V_4 and

TABLE 4. Regression analysis of vegetation age classes through time in the (A) LE, (B) ME, (C) UE, and (D) QU study reaches. Surface categories were channel (C), surface <5yrs old (V_1), surface 5-25 yrs old (V_2), surface 25-75 yrs old (V_3), and surface >75 yrs old (V_4).

	C	V_1	V_2	V_3	V_4
LE	0.7974 (P<0.05)	ns	0.7831 (P<0.05)	0.8559 (P<0.01)	0.9519 (P<0.001)
ME	ns	ns	ns	0.8431 (P<0.01)	0.9128 (P<0.005)
UE	ns	ns	ns	ns	ns
QU	ns	ns	ns	ns	ns

decrease in V_3 for both dam influenced reaches; additionally, the decrease in classes V_2 and C were significant in the LE (Table 4). Neither of the reference reaches exhibited statistically significant trends in vegetation age composition throughout our time series (Table 4).

In riffles with an equivalent slope-width index, the LE and ME reaches had a lower percentage of particles <128 mm relative to mainstem and side channel sites located in reference reaches (Figure 4). Differences in proportions of particles <64 mm or <256 mm were less distinct among reaches, so we do not report them here. Mainstem channels had a lower percentage of particles <128mm diameter than their adjacent side channels for all reaches (Figure 4). Bed material was generally coarsest near the dams and decreased in size with distance downstream. This trend was evident in both mainstem and side channel habitats where the proportion of particles >128 mm decreased as distance downstream of dams increased (Figure 5).

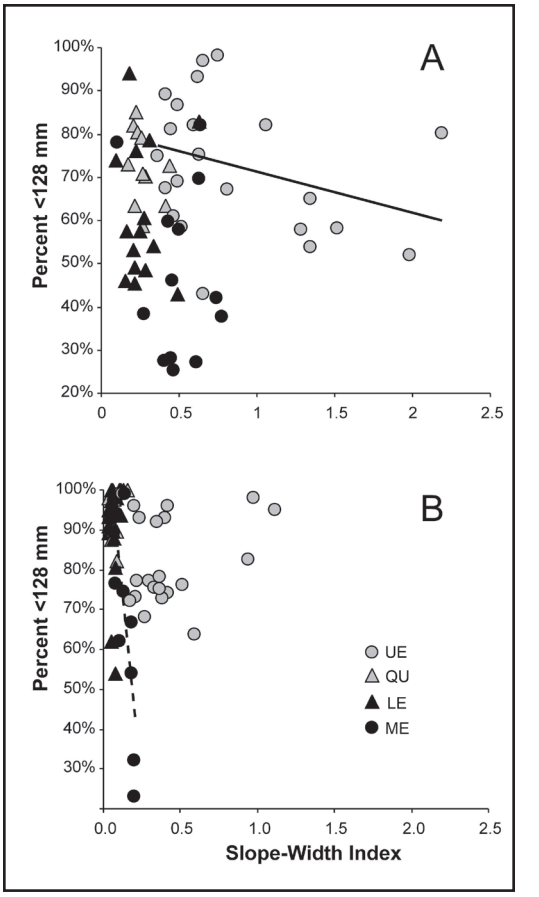

Figure 4. Percent of particles <128 mm diameter was generally lower in riffles below dams (LE and ME) than in riffles in reference reaches (UE and QU) for a given slope-width index. (A) mainstem riffles, (B) side channel riffles. The solid line indicates a statistically significant (P < 0.05) decline in the percent of particles <128 mm diameter in the UE. The dashed line indicates a significant decline in the percent of particles <128 mm diameter in the ME.

Discussion

Effects of Dams on Floodplain Age Structure

Analysis of aerial photographs made it possible to examine the effects of the two Elwha dams on historical and current floodplain dynamics. Temporal analysis of vegetation age classes showed that the mean age of all floodplain surfaces did not change through time in either regulated or unregulated reaches. However, the percentage of older floodplain surfaces (>75 yrs old) increased in the two reaches below dams, whereas the percentage of younger surfaces (<75 yrs old) decreased. These temporal trends were not detected in the

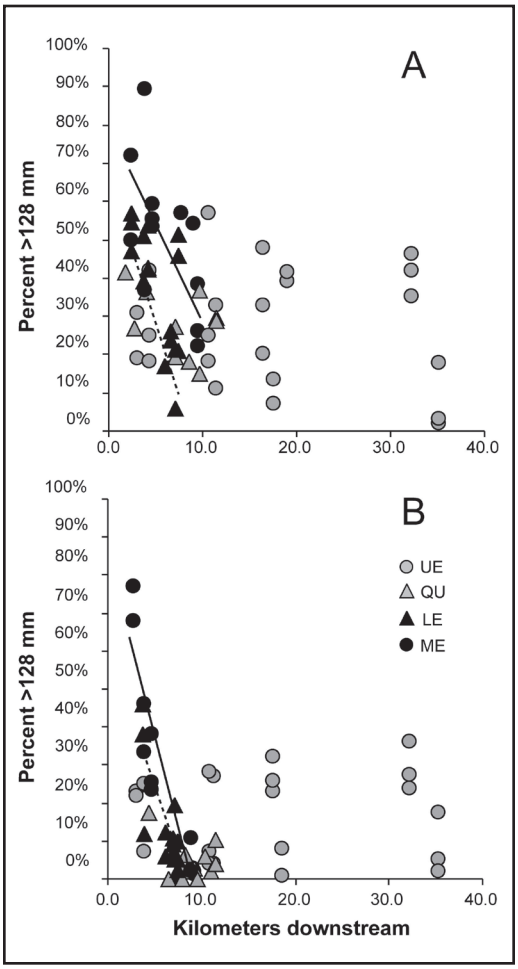

Figure 5. Trends in percent of particles >128 mm against distance downstream for (A) mainstem riffles and (B) side channel riffles. Solid lines indicate statistically significant ($P < 0.05$) downstream declines in percent of particles >128 mm diameter in the ME. Dashed lines indicate significant downstream declines in percent of particles >128 mm diameter in the LE. There were no statistically significant downstream trends in particle sizes in the UE and QU reference reaches.

unregulated reaches (Figure 3). Surface age trends exhibited by the regulated reaches indicated a divergence from the "shifting-mosaic-steady-state" model (Ward and Stanford 1983; Arscott et al. 2002), which characterizes the floodplain of the two reference reaches. That is, dynamic floodplain reaches typically maintain relatively constant age structure through time, but the dams have reduced sediment supply and set in motion a gradual transition toward a floodplain system dominated by mature forests and channels with relatively few intermediate-age surfaces. This shift indicates that river-floodplain dynamics below the dams are decreasing in severity and frequency.

Comparative Analysis of Floodplain Patch Dynamics

Using methods similar to those employed by Hohensinner et al. (2005), our study recreated historical floodplain surface age. However, unlike our use of reference reaches to provide a means of comparison, Hohensinner et al. (2005) studied a single 10-kilometer reach both before and after human channelization, rather than impoundment. Despite these differences, Hohensinner et al. (2005) found similar trends to those we found in the Elwha. Analysis of turnover rates from one habitat type to another prior to channelization showed no significant trends between habitat types, indicating the active floodplain had reached a state of equilibrium. The same transition analysis conducted after channelization produced a significant increase in the percent of succession to older habitat types. The reference or pre-channelization analysis and regulated or post-channelization analysis produced similar results to those based on the respective Elwha reaches.

Effects of Dams on Bed Material Grain Size Distributions

We found that particle size in ME and LE decreased as distance downstream from the dams increased (Figure 5). This trend was significant in both mainstem and side channel habitats. Additionally, relation of slope-width index to percent particles <128 mm (Figure 4) illustrated differences in particle size composition between dammed and reference reaches. At similar slope-index values, both reaches downstream of the dams had lower percentages of smaller particle sizes in comparison to the two reference reaches. These differences suggest that the river has retained its ability to mobilize particles up to 128 mm in diameter downstream of the dams and that reduction in supply of sediment has caused winnowing of sediments <128 mm from reaches downstream of the dams (Pohl 2004). In other words, sediments <128 mm in diameter have been gradually transported down river, and the lack of sediment influx from upstream results in bed compositions dominated by coarse cobble and boulder deposits.

We also identified statistically significant longitudinal trends in bed material sizes in both mainstem and side channel habitats below the dams. Bed material in both the ME and LE reaches were coarsest near the dams, and decreased in size with increasing distance from the dam. This trend is largely due to the recruitment of significant quantities of sand and gravel from the floodplain and adjacent terraces as the river erodes into these older deposits. Hence, the winnowing of particles <128 mm in diameter from below-dam river beds has been partially countered by recruitment of sand and gravels from adjacent landforms. Because total sediment recruitment increases in the downstream direction, the bed material becomes progressively finer.

Predicted Effects of Sediment Migration on Floodplain Age Structure and Bed Material Size

According to the Bureau of Reclamation (1996b) the initial influx of fine sediment after dam removal (2-5 yrs post-removal) is predicted to cause minimal bed aggradation, whereas the long-term aggradation of coarser gravel-sized sediment (>50 yrs post-removal) is likely to raise the river bed a meter or more. In addition, the BOR report suggests that the ME and LE reaches will respond differently with the most aggradation occurring in the lower reach because channel slope is less. Hence this reach has a lower sediment-transport capacity. We discuss responses of each reach separately.

In the ME reach, limited bed mobility (Pohl 2004) combined with a greater proportion of older forests on the floodplain will likely lead to minimal new channel building in response to the initial influx of fine sediments (2-5 yrs after removal). Fine sediment will move relatively rapidly through the reach, aggradation will be minimal, and bed material grain size distributions will likely be bi-modal and dominated by sand and boulders. Hence, channel migration will likely be limited to relict channels and low floodplain areas with young vegetation, while older floodplain surfaces would likely persist. However, channel migration in response to large woody debris (LWD) may be significant because LWD changes flow direction, traps sediment and creates new surfaces (Fetherston et al. 1995, Abbe and Montgomery 1996). These wood-related mechanisms could be increasingly influential given the rising proportions of mature trees found in the dam influenced reaches; more than forty percent of the ME is composed of late successional vegetation. Additionally, LWD inputs may be accelerated if overbank sediment deposition is substantial enough to bury, and subsequently kill, trees located on the floodplain (Acker et al. 2008). Loss of trees in this manner would most likely occur after several decades when bed aggradation increases in response to the influx of coarse sediment. Although some tree burial may also occur during the pulse of fine sediment following dam removal, we suspect these occurrences will be localized.

In subsequent decades (up to 50 yrs after dam removal), bed aggradation is predicted to gradually increase by an estimated 1 m or more as larger particles make their way downstream (BOR 1996b). This wave of coarse sediment is likely to reverse the stabilizing trend in channel-floodplain dynamics, which will result in significant channel building and surface age diversification. When sediment supply to the ME returns to relatively natural levels after several decades, we expect channel patterns and channel-floodplain dynamics will resemble conditions similar to those found in the QU reference reach or in similar island-braided reaches elsewhere in the Cascade and Olympic Mountains of western Washington (O'Connor et al. 2003; Beechie et al. 2006). In island-braided channels, the middle age classes comprise a significant proportion of the floodplain, whereas current age distributions in the ME resemble those of stable straight channels (Beechie et al. 2006). Hence, increased sediment supply and the potential for significant recruitment of LWD may transform the simplified ME reach into a network of varying patch ages, eventually resembling the "shifting-steady-state mosaic" analogues of gravel-bed island-braided systems.

The physical characteristics of the LE differ from the ME reach and the other two reaches. Though LE is downstream of both dams, lateral migration and erosion of older surfaces is presently occurring, creating a more diverse floodplain than one might expect given a dramatically reduced upstream sediment supply. Moreover, bed material in the LE has become only slightly armored as a result of sediment limitation (BOR 1995, Pohl 2004) and bed material is still mobilized by two to 10 year flood events. In this reach, the initial influx of fine sediments eroded from reservoir deposits (2-5 yrs after dam removal) will fill pools and only

slightly aggrade riffles (BOR 1996b). As a result, bed material composition immediately downstream of the dam will likely become bi-modal, with high proportions of sand and boulders but relatively little gravel. Therefore, the LE reach will likely experience little increase in channel migration and little change to floodplain age structure in the near term. After several decades, the sediment supply will become gravel-dominated (BOR 1996b), aggradation of the mainstem channel will likely cause channel migration and activation of existing side channel habitats, and bed material size composition will resemble those of the reference reaches. As a result, the LE will likely experience several decades of increasing lateral migration, erosion of some mature forest proportions of the floodplain, and an increased proportion of young floodplain surfaces. This transition from older surfaces to more intermediate age surfaces may cause floodplain age structure to shift from one that currently is quite typical of island-braided channels, toward a more braided channel pattern (Knighton and Nanson 1993). Channel migration in response to bed aggradation could also increase LWD recruitment from older floodplain surfaces, and overbank deposition of fines on older surfaces could increase tree mortality as a result of burial.

Conclusion

We documented gradual stabilization of floodplain surfaces downstream of the Elwha dams over the past 60 years, as well as coarsening of bed material relative to reference reaches. Both are effects of the interruption of sediment supply to reaches downstream of the dams. Removal of the two dams will release stored fine sediment, initially creating bi-modal grain size distributions in reaches downstream of the dams and perhaps slightly increasing channel migration and erosion of floodplain surfaces. In subsequent decades, gravel bed load supply will increase and gradually return to natural levels, aggrading river beds approximately 1 m. We predict that this aggradation will significantly increase lateral channel migration and erosion of floodplain surfaces, gradually shifting floodplain age distributions towards younger age classes. Once sediment supply is similar to that of undammed reaches, river-floodplain dynamics will resemble those of other island-braided reaches in the Olympic and Cascade Mountains of western Washington, with relatively even distributions of age classes on the floodplain.

Acknowledgements

We thank George Pess (NOAA) for assisting with the study design, data collection, and peer review process; Mike McHenry, Mel Elofson, Raymond Moses, Sonny Sampson and the Elwha Tribe for field assistance, advice and access to Tribal land; and Casey Rice and Frank Sommers (NOAA) for peer review. Karrie Hanson, Martin Liermann, Todd Bennett, Deborah Harstad, Vija Pelekis, Ranae Holland, Correigh Greene, Chau Tran, Kerri Haught and Adam Goodwin (NOAA); and Junko Harbrod and Sasha Aurora (Peninsula College); all contributed long hours collecting and processing field data. Additionally, Ashley Green, Matt Groce and Amy Newman of the USGS, Western Fisheries Research Center expended considerable effort collecting and processing all field data from the upper Elwha watershed. The use of trade, firm, or corporation names in this publication is for the information and convenience of the reader. Such use does not constitute an official endorsement or approval by the U.S. Government of any product or service to the exclusion of others that may be suitable.

Literature Cited

Abbe, T. B. and D. R. Montgomery. 1996. Large woody debris jams, channel hydraulics, and habitat formation in large rivers. Regulated Rivers: Research and Management 12:201-221.

Acker, S. A., T. J. Beechie, and P. B. Shafroth. 2008. Effects of a natural dam-break flood on geomorphology and vegetation on the Elwha River, Washington, U.S.A. Northwest Science 82 (Special Issue):210-223.

Beechie, T. J., M. Liermann, M. M. Pollock, S. Baker, and J. Davies. 2006. Channel pattern and river-floodplain dynamics in forested mountain river systems. Geomorphology 78:124-141.

Booth, D. E. 1991. Estimating prelogging old-growth in the Pacific Northwest. Journal of Forestry 89(10):25-29.

BOR (Bureau of Reclamation). 1995. Alluvium distribution in Lake Mills, Glines Canyon project and Lake Aldwell, Elwha Project. Elwha Technical Series PN-95-4. United States Department of Interior, Pacific Northwest Region, Boise, ID.

BOR (Bureau of Reclamation). 1996a. Removal of Elwha and Glines Canyon Dams. Elwha Technical Series PN-95-7. United States Department of Interior, Pacific Northwest Region, Boise, ID.

BOR (Bureau of Reclamation). 1996b. Sediment analysis and modeling of the river erosion alternative. Elwha

Technical Series PN-95-9. United States Department of Interior, Pacific Northwest Region, Boise, ID.

Fetherston, K. L., R. J. Naiman, and R. E. Bilby. 1995. Large woody debris, physical process, and riparian forest development in montane river networks of the Pacific Northwest. Geomorphology 13:133-144.

Franklin, J. F. and C. T. Dyrness. 1973. Natural vegetation of Oregon and Washington. USDA Forest Service General Technical Report PNW-8. Pacific Northwest Forest and Range Experiment Station, Portland, OR.

Grant, G. E., J. C. Schmidt, and S. L. Lewis. 2003. A geomorphological framework for interpreting downstream effects of dams on rivers. *In* G. E. Grant and J. E. O'Connor (editors)**,** A Peculiar River: Geology, Geomorphology, and Hydrology of the Deschutes River, Oregon. Water Science and Application 7, American Geophysical Union, Washington, DC. Pp. 209-225.

Hohensinner, S., G. Haidvogl, M. Jungwirth, S. Muhar, S. Preis, and S. Schmutz. 2005. Historical analysis of habitat turnover and age distributions as a reference for restoration of Austrian Danube floodplains. Transactions on Ecology and the Environment 83:1743-3541.

Knighton, A. D. and G. C. Nanson. 1993. Anastomosis and the continuum of channel pattern. Earth Surface Processes and Landforms 18:613-625.

Leopold, L. B., M. G. Wolman, and J. P. Miller 1964. Fluvial processes in geomorphology. Dover Publications, Inc., New York.

Ligon, F. K., W. E. Dietrich, and W. J. Trush. 1995. Downstream ecological effects of dams: a geomorphic perspective. Bioscience 45:183-192.

O'Connor, J. E., M. A. Jones, and T. L. Haluska. 2003. Flood plain and channel dynamics of the Quinault and Queets Rivers, Washington, USA. Geomorphology 51:31-59.

Pielou, E. C. 1977. Mathematical Ecology. John Wiley and Sons, Toronto, ON, Canada.

Pizzuto, J. 2002. Effects of dam removal on river form and process. Bioscience 52:683-691.

Pohl, M. P. 2004. Channel bed mobility downstream from the Elwha Dams, Washington. The Professional Geographer 56:422-431.

Richards, K. 1982. Rivers: Form and process in alluvial channels. Methuen, Inc., New York.

Tabor, R. 1975. Guide to the Geology of Olympic National Park. University of Washington Press, Seattle.

USACOE. 1993. HEC-6 software for estimating scour and deposition in rivers and reservoirs. US Army Corps of Engineers Hydrologic Engineering Center, Davis, CA.

US Geological Survey (USGS). 1996. Standards for Digital Orthophotos, Part 2: Specifications. National Mapping Division Technical Instructions.

Wolman, M. G. 1954. A method of sampling coarse river-bed material. Transactions of the American Geophysical Union 35:951-956.